It is readily seen that rays, emanating at an arbitrary angle θ from a point source, after being diffracted by the grating to several orders (having angles $n\lambda/p$) virtually meet on circles at a distance l from the grating. The radii of the circles in the small-angle approximation are $nl\lambda/p$. In case of polychromatic light, color rings will appear at each point on the grating. Rays emanating from all the virtual circles are crossed and are, therefore, insensitive to the distance of the observer from the grating. But if the point source and the center of the grating are not aligned with the eye (see Fig. 4), the diffraction pattern will not retain its circular symmetry but will instead spread into a butterfly shape. To elucidate this point let us suppose that the eye is very far from the grating's center but very close to the grating. Since the pupil is small compared to the radius of the circles of the grating, at this location the diffraction pattern can be considered a linear grating (Fig. 4). Therefore, the diffraction pattern forms a virtual array of dots. In any intermediate case we have contributions in several directions. These directions determine the butterfly angle β shown as heavy crossed lines in Fig. 4. When the pupil (white circle) adjusts itself to the available light, an observation of this butterfly angle will be made only when

$$\beta < 2\sin^{-1}(r_1/\delta), \tag{3}$$

where δ is the shift of the center of the pupil from the center of the grating. While we align the sight we cannot measure this angle precisely but we can tell whether the inner circle is complete or broken. If it is broken, it means that we are off-center at least by one radius of the pupil. Thus the effective peephole radius in analogy with the other sights discussed is the radius of the pupil which adjusts itself to illumination conditions.

In brief, we suggest use of a circular diffraction grating instead of a peephole as a night sight. This sight has the following advantages:

(1) It obstructs a relatively small portion of the available target light.

(2) It is insensitive to the distance between the eye and grating. Therefore, the eye can be at a distance from the grating. (This may be useful for pistols and certain optical devices.)

(3) The efffective peephole is determined by the pupil of the eye which automatically adjusts itself to the illumination conditions.

(4) The eye must be focused on two objects only: the foresight and target aimed at.

The disadvantages of this sight are:

(1) It is more fragile than the peephole or V-groove sight.

(2) The sight might be inferior to peephole or V-groove sight during the daytime.

We thank J. Fewerlich, A. Kerman, I. Glatt, and E. Keren for their help. O.K. thanks L. Horowitz for useful comments and discussions.

References

1. Bureau of Naval Personnel, *Principles of Naval Ordnance and Gunnery* (Washington, D.C.).

Solar magnetic and velocity-field measurements: new instrument concepts; errata

Jan O. Stenflo

Swiss Federal Institute of Technology, Institute of Astronomy, ETH-Zentrum, CH-8092 Zurich, Switzerland.
Received 30 May 1984.
0003-6935/84/193267-01$02.00/0.

Four equations in this paper[1] were misprinted; they should read as follows:

$$M_p = \tfrac{1}{2}\begin{pmatrix} 1 & 1 & 0 & 0 \\ 1 & 1 & 0 & 0 \\ 0 & 0 & 0 & 0 \\ 0 & 0 & 0 & 0 \end{pmatrix}, \tag{5}$$

$$M_{1,2} = \tfrac{1}{2}\begin{pmatrix} 1 & \pm 1 & 0 & 0 \\ \pm 1 & 1 & 0 & 0 \\ 0 & 0 & 0 & 0 \\ 0 & 0 & 0 & 0 \end{pmatrix}, \tag{6}$$

$$M_\omega(A) = 2J_1(A)\begin{pmatrix} 0 & 0 & 0 & 0 \\ 0 & 0 & 0 & 0 \\ 0 & 0 & 0 & 1 \\ 0 & 0 & -1 & 0 \end{pmatrix}, \tag{15}$$

$$M_{2\omega}(A) = 2J_2(A)\begin{pmatrix} 0 & 0 & 0 & 0 \\ 0 & 0 & 0 & 0 \\ 0 & 0 & 1 & 0 \\ 0 & 0 & 0 & 1 \end{pmatrix}. \tag{16}$$

Reference

1. J. O. Stenflo, "Solar Magnetic and Velocity-Field Measurements: New Instrument Concepts," Appl. Opt. 23, 1267 (1984).

Extreme UV measurements of a varied line-space Hitachi reflection grating: efficiency and scattering

Jerry Edelstein, Michael C. Hettrick, Stanley Mrowka, Patrick Jelinsky, and Christopher Martin

University of California, Space Sciences Laboratory, Berkeley, California 94720.
Received 22 June 1984.
0003-6935/84/193267-03$02.00/0.

Mechanically ruled aberration-corrected gratings have been proposed for a variety of spectrographs.[1-5] At grazing incidence, the improvements in imaging which can be realized in this manner are substantial,[3-5] allowing for the first time high-resolution spectroscopic studies in the extreme UV and soft x ray. In addition, varied groove spacings offer advantageous spectral noise characteristics. Energy scattered from periodic ruling errors should be distributed throughout the dispersion plane rather than concentrated into false spectral images (e.g., ghosts).

We present the first extreme UV measurements of a grating which has been mechanically ruled with smooth variations in the grating constant. The grating was supplied by Hitachi, Ltd. and was designed for a flat-field spectrometer covering

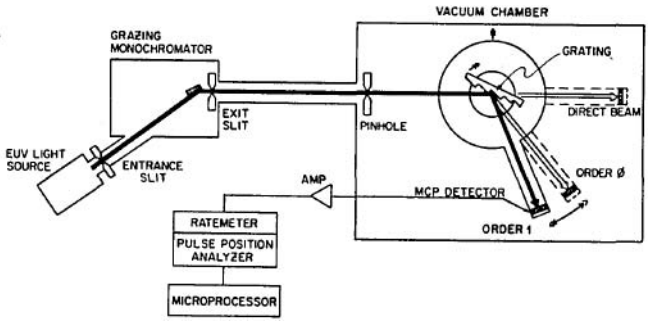

Fig. 1. Schematic diagram of test apparatus. Double arrows signify mechanical adjustments.

Table I. Absolute Efficiency vs Wavelength

Wavelength (Å)	Zero order[a] (%)	First order[a] (%)	Second order[a] (%)
68	24	8.5	
170	56	12.0	<1
256	57	10.2	0.6
304	62	7.7	0.3
584	72	7.6	1.5
1216	85	1.0	

[a] Relative measurement error = ±5%.

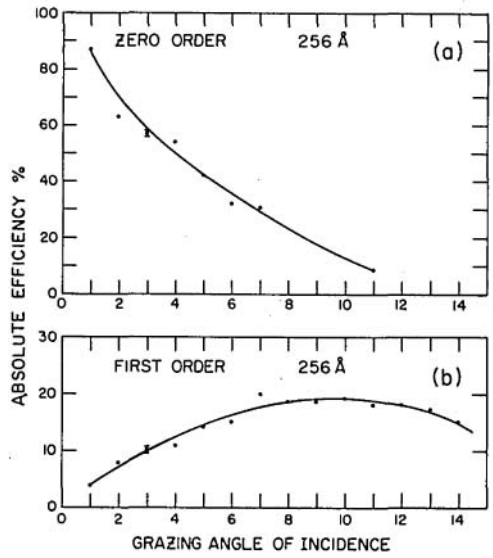

Fig. 2. Measured absolute grating efficiency at λ = 256 Å as a function of incident angle measured from grating tangent. Error bars arise predominantly from uncertainties in background removal: (a) zero order; (b) first order.

the 50–300-Å region. The imaging properties of that instrument are described by Kita *et al.*[6] The nominal grating line spacing is 1200 lines/mm and varies from 1015 to 1449 lines/mm across a 50-mm ruled width. The grooves are 30 mm long and blazed at an angle of 3.2°. Measurements were made using a gold replica having a spherical surface of 5649-mm radius.

A schematic of the testing apparatus is shown in Fig. 1. Lines in the extreme UV were generated with a hollow cathode gas discharge lamp[7] (256, 304, 584, 1216 Å) and a Henke tube[8] (68, 170 Å). The light entered a McPherson 2.2-m monochromator, exiting with an f ratio of ~40. This beam was aperture-stopped by a pinhole or slit, which fed the grating with a highly collimated beam ($f > 700$). The grating and detector were mounted on concentric turntables placed on a manipulator which provided motion perpendicular to the incident beam. The grating was mounted approximately in-focus as described by Kita,[6] 237 mm from the entrance pinhole. Typically, the inside first spectral order was used, requiring the grating blaze angle to trail in the direction of the incident beam. The detector could be rotated within the dispersion plane at a distance of 235 mm from the grating center. A microchannel plate detector was used providing photon-counting and 2-D imaging. The detector pores were biased 20° from the normal of the beam to minimize the variation of detector efficiency due to the incident angle.

The intensity of the incident beam was monitored by direct illumination of the detector. To obtain the absolute grating efficiency, the grating was translated into the beam, and the detector was rotated into the diffracted order of interest. To minimize the effect of spatial variations in detector efficiency, the image intensity was always measured at the same location on the microchannel plate. Spectral impurities from the monochromator were removed by subtraction of off-line counts. Closing the monochromator exit slit also allowed independent monitoring of the detector background, which was found to be small (~8 counts/sec across the detector active area of 25 × 25 mm). Count rates for the beams were in the 1000–15,000-count/sec range, the highest rates requiring electronic dead-time corrections of ~25%.

Table I reports the results for absolute grating efficiency vs wavelength measured at 68, 170, 256, 304, 584, and 1216 Å. The angle of incidence was 87°, for which the theoretical first-order efficiency at the grating center peaks at a blaze wavelength of 100 Å. The reflection graze angle relative to the grating facets is 6.2°, for which the reflectance of the gold surface is estimated to be 65%. The groove shadowing is significant in this mounting; geometrical calculations[9] suggest 30% groove efficiency near the blaze. Thus the predicted absolute grating efficiency in first order is 20%. The measurements reveal a 12% absolute efficiency at 170 Å and a very broad blaze function which extends over several hundred angstroms with usable efficiency. Thus, at 170 Å, in excess of 60% of the theoretical efficiency has been recovered. The lower efficiency at 68 Å is attributed to both the lower reflectance and the rapid decline expected in the blaze function shortward of 100 Å. The measured zero-order efficiency shows the expected decrease toward the shorter wavelengths. Near the blaze, ~75% of the reflected light goes into zero order, as expected on the basis of groove shadowing.

Figure 2 shows the results of 256-Å measurements at different angles of incidence. This was done to more accurately constrain the blaze function. A 330-μm pinhole was used to keep the grating underilluminated at the lowest graze angles of incidence (1°). At these shallow angles, the first-order efficiency is attenuated by groove shadowing, which is found to result in a significant zero-order intensity. The graze angle of incidence for which λ256 Å is formally blazed is 12.75°; thus the efficiency rises toward these steeper graze angles. However, prior to the blaze the reflectance begins to dominate and causes a turnover at 10°. At this angle, the blaze wavelength is 212 Å, and the blaze efficiency is estimated[9] to be 27%, including a reflectance of 45% at the facet graze angle of 13.2°. The measured efficiency of 19% at 256 Å represents 70% of the theoretical efficiency in first order.

Efficiency measurements were also made as a function of

position across the ruled width at 256 Å and a 87° incident angle. The spot sizes were ~6 mm in the ruling direction. Smooth monotonic changes were measured in both the first-order (8.5–11.6%) and zero-order (59.8–52.8%) efficiencies across 40 mm, wherein the line density varied from ~1400 to 1050 lines/mm. These variations are attributed to the expected shift in the blaze wavelength toward 256 Å as the line density decreases. Shifts in the blaze wavelength due to curvature of the grating surface were calculated and found to be negligible. However, the effects of grating groove profile on these measurements cannot easily be deconvolved. Such effects could arise from groove imperfections, which become more important at the higher line densities, and wear in the diamond tool during the ruling process.

Scattering measurements were performed via computer acquisition of the diffracted image profiles. No dead-time corrections were applied, as these would be uniform from pixel to pixel and thereby not change the relative efficiency scale. An entrance slit of 220-μm width spread over a 6% variation in-line spacing on the grating. Figure 3 shows histograms of the results for 304 Å, plotted for each detector pixel (100 μm) along the dispersion direction. In first order, each pixel represents ~1 Å. Due predominantly to the finite entrance slit width, the 304-Å first-order image shows a FWHM resolution of ~5 Å. No ghost images were detected above the background of scattered light. At a detector pixel 50 Å from the first-order 304-Å image, this measurement limit was $5 \sim 10^{-5}$ of the parent line intensity. The absence of ghosts was also evident in a visible laser light (6328 Å), which also revealed a large decrease in the level of focused stray light in comparison to conventionally ruled gratings of the same line density.

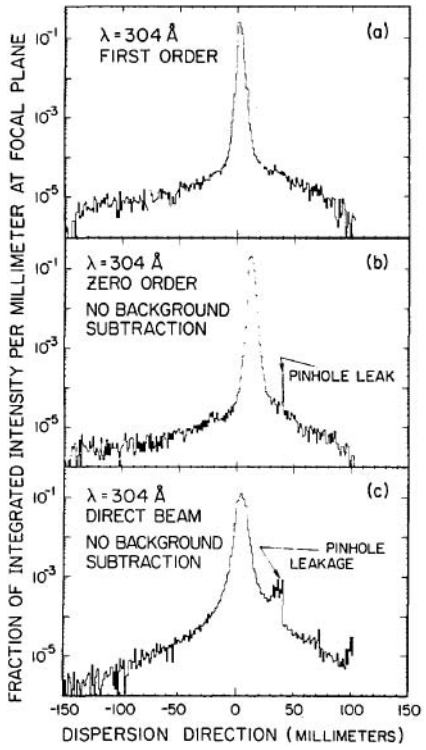

Fig. 3. Image profiles at λ = 304 Å in the dispersion direction. Resolvable detector bins are 0.1 mm: (a) in the vicinity of first order, (b) in the vicinity of zero order, (c) image of entrance slit (220-μm width).

Figure 3(a) also shows the level of focused stray light in the extreme UV to be very small. At a detector pixel which lies 50 Å away from the diffracted position for first-order 304 Å, the stray light is measured to be $\sim 10^{-5}$/Å of the parent line. Similar profiles were obtained using first-order 256-Å light. Figure 3(c) shows an image of the direct 304-Å beam revealing diffraction from the entrance slit. As the concave grating is used approximately in-focus, slit diffraction should not broaden images off the grating. However, a similar image profile at the detector is expected to result from diffraction at the grating aperture. Although a direct comparison to Fig. 3(a) cannot be made, the comparatively broad wings of the first-order profile indicate the presence of stray light from the grating. Similar broad wings for the zero-order profile [Fig. 3(b)], which is strictly independent of groove locations, suggest a contribution from groove surface irregularities.

These measurements compare well with the best previous measurement at λ1236 Å for a 313-line/mm ruled grating,[10] where a similar level of stray light was measured. The very low level of stray light for our 1200-line/mm ruled grating at λ304 Å is attributed to the optical–mechanical system which was used to control fine incremental variations (0.2 Å) in the groove spacings.[6] The use of a specially designed cylindrical tool guide also was responsible for the absence of concentric irregularities on the concave ruled surface and their contribution to scattered light. Compared to conventional ruling engines, whose noise level is of the order of 30 Å, random errors in the line spacings should be significantly smaller. As such errors are believed to be largely responsible for the level of focused stray light, one expects a corresponding reduction in the level of stray light from gratings ruled in such a manner. The amplitude of periodic errors in the groove spacings should also decrease and assist in the attenuation of ghost intensities.

Moreover, the peak intensity of ghosts in an actual spectroscopic mount, where a large section of the ruled width is illuminated, should be even smaller. Consider the mth order Rowland ghost of a parent line. Its position is given by the simple formula

$$\lambda_{\text{ghost}}/\lambda_{\text{parent}} - 1 = \pm md/P, \tag{1}$$

where d is the line spacing and P is the period of the screw/bearing mechanism assumed to introduce a harmonic variation in the line spacing. For a 50% variation in line spacing d across the grating, the width of these ghosts should spread over half of the spectral distance to the parent line ($2\Delta\lambda_{\text{ghost}} \simeq \lambda_{\text{ghost}} - \lambda_{\text{parent}}$). Thus constructive interference is prevented, and any such ghosts should blend into the general background of stray light.

The authors would like to thank T. Harada for supplying the varied line-space grating on which the above tests were performed. We also acknowledge helpful discussions with B. Bach, S. Bowyer, and R. Malina. This work was supported by NASA contract NASW-3636.

Patrick Jelinsky and Christopher Martin also hold appointments in the Department of Physics.

References

1. M. V. R. K. Murty and N. C. Das, "Narrow-band Filter Consisting of Two Aplanatic Gratings," J. Opt. Soc. Am. **72**, 1714 (1982).
2. J. D. Baumgardner, "Theory and Design of Unusual Concave Gratings," Thesis, U. Rochester (1969).
3. T. Harada and T. Kita, "Mechanically Ruled Aberration-Corrected Concave Gratings," Appl. Opt. **19**, 3987 (1980).

4. D. E. Aspnes, "High-Efficiency Concave-Grating Monochromator with Wavelength-Independent Focusing Characteristics," J. Opt. Soc. Am. **72,** 1056 (1982).
5. M. C. Hetrick and S. Bowyer, "Variable Line-Space Gratings: New Designs for Use in Grazing Incidence Spectrometers," Appl. Opt. **22,** 3921 (1983).
6. T. Kita, T. Harada, N. Nakano, and H. Kuroda, "Mechanically Ruled Aberration-Corrected Concave Gratings for a Flat-field Grazing Incidence Spectrograph," Appl. Opt. **22,** 512 (1983).
7. F. Paresce, S. Kumar, and C. S. Bowyer, "Continuous Discharge Line Source for the XUV," Appl. Opt. **10,** 1904 (1971).
8. B. L. Henke and M. L. Tester, Adv. X-ray Anal. **18,** 76 (1975).
9. M. Neviere and W. R. Hunter, "Analysis of the Changes in Efficiency Across the Ruled Area of a Concave Diffraction Grating," Appl. Opt. **19,** 2059 (1980).
10. G. H. Mount and W. G. Fastie, "Comprehensive Analysis for Gratings for Ultraviolet Space Instrumentation," Appl. Opt. **17,** 3108 (1978).

Patents *continued from page 3250*

4,430,659 7 Feb. 1984 (Cl. 346–135.1)

Protuberant optical recording medium.

K. N. MAFFITT, W. B. ROBBINS, and R. F. WILLSON. Assigned to Minnesota Mining and Manufacturing Co. Filed 13 Feb. 1981.

This invention describes an optical disk recording medium that allows the recorded information to be stored in the form of bubbles (protuberances) instead of the usual holes (pits). The medium contains a light absorbing film of amorphous carbon <60 nm thick and which is sufficiently plastic to allow plastic deformation on localized heating resulting from impingement by a focused laser beam to enable formation of the localized protuberances which can subsequently be optically detected and can be used as a master information record for replication purposes. R.A.B.

4,432,085 14 Feb. 1984 (Cl. 369–93)

Dual input telescope for multi-beam optical record and playback apparatus.

C. W. RENO and G. L. ALLEE. Assigned to RCA Corp. Filed 30 Oct. 1981.

This invention describes an optical system to be used for a multiple-beam optical disk recording system. The system includes an apparatus for splitting the output light beam of a single laser into a plurality of read and record light beams. These beams are recombined and directed along a common light path to an objective lens and focused onto the optical recording medium. The key to this invention is a dual-input lens beam-expansion telescope which is utilized with the beam combiner optics to provide the necessary expanded light beams which fill the entrance aperture of the objective lens. R.A.B.

4,435,041 6 Mar. 1984 (Cl. 350–162.24)

Chromatic aberration correction in a multiwavelength light beam deflection system.

E. J. TOROK and W. A. HARVEY. Assigned to Sperry Corp. Filed 28 May 1982.

A previous patent 3,752,563 described a magnetooptic light deflector 16 which deflected λ_0 by angle θ_0. To utilize such a magnetically controlled grating for a white light, it is necessary to devise a compound lens 18 of crown and flint glass which will correct the chromatic aberration caused by the grating, so that λ_0 and λ emerge from the lens parallel. A variety of lens systems are devised to accomplish this. E.D.P.

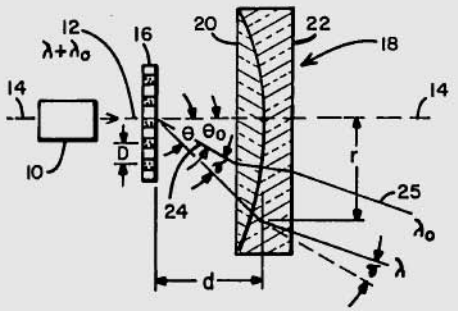

4,440,013 3 Apr. 1984 (Cl. 73–23.1)

Gas chromatograph, Fourier transform, infrared spectroscopy system.

G. E. ADAMS. Assigned to International Business Machines Corp. Filed 3 Mar. 1982.

This invention concerns an improvement to the sample-handling system of GC-IR instruments, primarily that of locating the IR light-pipe within the GC oven and injecting the effluent from the GC capillary directly into one end of the light-pipe in conjunction with a secondary sweep gas flow. It is claimed to reduce GC peak broadening or tailing. The twelve claims granted cover both FTIR and conventional IR applications as well as a number of variations on the detailed design. J.A.D.

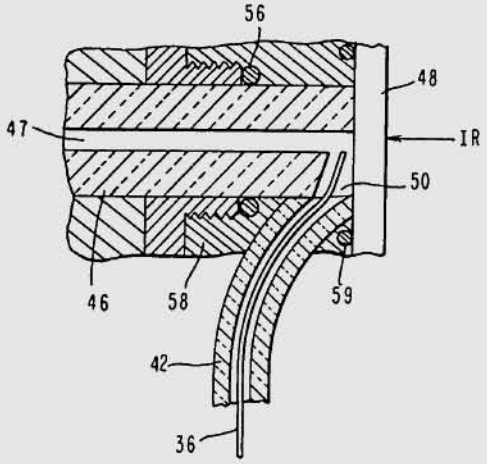

4,444,456 24 Apr. 1984 (Cl. 350–3.7)

Holographic method and apparatus for transformation of a light beam into a line source of required curvature and finite numerical aperture.

K. JAIN, M. R. LATTA, and G. T. SINCERBOX. Assigned to International Business Machines. Filed 23 June 1982.

This invention concerns a holographic technique to transform a collimated beam of light into a line source of arbitrary shape and *f*/No. The stated motive is to increase the efficiency of photolithographic techniques for microelectronics fabrication, but it would also have obvious application to spectrometry. The five claims granted cover the apparatus, the technique of making the hologram using a suitably shaped mask in one arm of a standard dual-path optical system, and a specific system having multiple sources of the same geometry but differing *f*/Nos. J.A.D.

4,445,749 1 May 1984 (Cl. 350–376)

Holographic products and processes.

S. A. BENTON. Assigned to Polaroid Corp. Filed 6 June 1980.

This invention covers a technique for making achromatic (or polychromatic) white-light holograms from a series of 2-D photographs. The method starts with a series of photographs of an object taken while translating the camera normal to its line of sight. The resulting photographs are then sequentially projected to make a series of strip holograms on a single medium inclined to the horizontal axis. This strip hologram is then projected to produce a second hologram on a medium inclined to the vertical axis. This second hologram, then, can be viewed in white light to produce an achromatic 3-D image or, alternately, by the proper use of filters, viewed in white light to produce a full-color 3-D image. J.A.D.

4,447,111 8 May 1984 (Cl. 350–3.7)

Achromatic holographic element.

K. G. LEIB. Assigned to Grumman Aerospace Corp. Filed 25 Feb. 1982.

This patent describes a process for producing holographic optical elements without chromatic aberration. The achromatic elements are fabricated by recording multiple holograms on the same recording medium. In each recording the reference angle and the object distance of the pinhole are adjusted for one particular wavelength. The problems related to cross talk among the multitude of reconstructed images from the hologram are not discussed. W.-H.L.

continued on page 3296